ADVANCED FUNCTIONAL MATERIALS
www.afm-journal.de

Two-Stage Reactive Polymer Network Forming Systems

*Devatha P. Nair, Neil B. Cramer, John C. Gaipa, Matthew K. McBride, Emily M. Matherly, Robert R. McLeod, Robin Shandas, and Christopher N. Bowman**

There are distinct advantages to designing polymer systems that afford two distinct sets of material properties– an intermediate polymer that would enable optimum handling and processing of the material, while maintaining the ability to tune in different, final polymer properties that enable the optimal functioning of the material. In this study, by designing a series of non-stoichiometric thiol-acrylate systems, a polymer network is initially formed via a base catalyzed Michael addition reaction that proceeds stoichiometrically via the thiol-acrylate "click" reaction. This self-limiting reaction results in a polymer with excess acrylic functional groups within the network. At a later point in time, the photoinitiated, free radical polymerization of the excess acrylic functional groups results in a highly crosslinked, robust material system. These two stage reactive thiol-acrylate networks that have intermediate stage rubbery moduli and glass transition temperatures that range from 0.5 MPa and −10 °C to 22 MPa and 22 °C, respectively, are formulated and characterized. The same polymer networks can then attain glass transition temperatures that range from 5 °C to 195 °C and rubbery moduli of up to 200 MPa after the subsequent photocuring stage. The two stage reactive networks formed by varying the stoichiometric ratios of the thiol and acrylate monomers were shown to perform as substrates for three specific applications: shape memory polymers, impression materials, and as optical materials for writing refractive index patterns.

1. Introduction

Numerous polymerization reactions used to form crosslinked polymer networks are extremely complex, often having an initial resin formulation that undergoes a rapid transition from a relatively low viscosity liquid state to a highly crosslinked, glassy solid state with corresponding changes observed in numerous material properties. The ability to react and form polymer networks with intimate control of the polymerization dynamics and the ultimate material properties has enabled their pervasive use across a broad spectrum of applications and contributed to significant technological advancements.[1–6] The wide range of fields in which polymer networks have become important vary from automobile and aircraft parts to biomedical devices to lithographic imprint materials and optical devices.[2–13] However, for many applications, it would be advantageous to have at least one stage of the polymerization occur through a self-limiting polymerization reaction that forms a stable polymer network with desirable physical attributes that simultaneously maintains the ability, upon application of a second stage curing stimulus, to react further and achieve a second and final set of material properties. Such a system enables the achievement of two distinct and largely independent sets of material properties as might be necessary for multiple stages in the processing and life-cycle of certain applications.

Here, we introduce a polymer system that is formed by two reactions capable of generating distinct first and second stage polymers. The first stage polymer takes advantage of the powerful capabilities afforded by the "click" reaction paradigm to engender a specific, self-limiting reaction that is orthogonal to the desired second stage reaction.[6] While multiple approaches are possible using a variety of reactions, here, we specifically implement the thiol-acrylate Michael addition reaction as the click reaction of choice.[4,7–10] When a mixture of a multifunctional thiol and excess multifunctional acrylate undergoes this reaction, a stoichiometric, self-limiting reaction between the thiol and acrylate functional groups occurs. This approach leaves whatever acrylates were present in excess within the initial formulation as unreacted acrylic functional groups within an otherwise stable polymer network. In the second stage, in the presence of a photoinitiator and light, the remaining acrylic moieties polymerize to increase the crosslink density significantly wherever and whenever the light is used (**Scheme 1**).

A number of other reactions could readily be used in the first stage including alcohol/isocyanate or thiol/isocyanate reactions to form urethane or thio-urethane linkages or alkyne-azide reactions to form a triazole-containing network.[3] For these initial reactions second stage curing is desirably initiated by light exposure to facilitate stability of the initially cured network. Hence, at the completion of stage one and with appropriate selection of monomers, the initial network contains photoreactive, polymerizable moieties such as the acrylates used here or methacrylates, epoxies, or thiols and enes that could

D. P. Nair, N. B. Cramer, J. C. Gaipa, M. K. McBride, E. M. Matherly, Prof. R. R. McLeod, R. Shandas, Prof. C. N. Bowman
Department of Chemical and Biological Engineering
Campus Box 424, ECCH 126
University of Colorado
Boulder, CO 80309-0424, USA
E-mail: christopher.bowman@colorado.edu

DOI: 10.1002/adfm.201102742

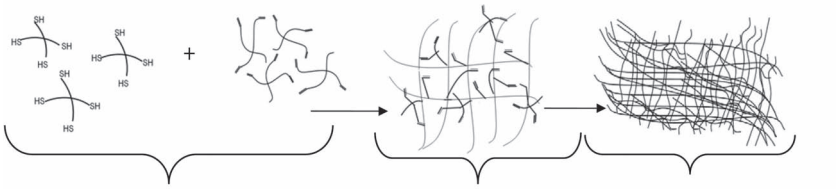

Scheme 1. Methodology for dual-network forming thiol-acrylate systems.

participate in the thiol-ene reaction. Here, to avoid the necessity of producing monomers that would need to be functionalized with multiple types of chemical functionalities, we chose to use the thiol-acrylate Michael addition and photoinitiated radical-mediated acrylic polymerization so that the acrylate monomers, when used in excess, would directly participate in both reactions. This approach guarantees the simplest monomer selection and development, takes advantage of the orthogonal nature of the thiol-acrylate Michael addition, and assures to the extent possible that an overwhelming fraction of the initial monomer will be bound into the network at the end of the stage one reaction.

In particular, the thiol-acrylate reaction exhibits a wide range of application versatility due to the multitude of available thiol and acrylate monomers as well as the ability to react by Michael addition reactions or free radical polymerizations.[4,7–11] The Michael addition reaction between a thiol and an acrylate enables the thiol and acrylic monomers to react under relatively facile reaction conditions to yield crosslinked polymer networks. The Michael addition reaction has been shown to progress robustly to completion under a wide range of conditions that facilitate numerous options with respect to monomer selection, reaction temperature and the presence or absence of solvents, all resulting in sophisticated, uniform polymer networks.[7–11] Additionally, the ability of Michael addition reactions to favor complete conversion and rapid cure rates at ambient temperature have made these polymer systems an ideal choice for applications that vary from industrial coatings to drug delivery as well as cell scaffolds and crosslinked hydrogels.[4,13–15] It is well known that in conventional network-forming resins the stoichiometry of the monomers used to form the thiol-acrylate Michael addition networks must be 1:1 to form completely reacted networks.[4,8]

The two-stage reactive polymer network forming system is extremely versatile as simple and judicious variations in the choice of thiol and acrylate monomer types, functionality, and stoichiometric ratios enable a nearly limitless range of initial and final properties. The range of possibilities for this dual cure approach is illustrated herein by developing approaches suitable for three distinct applications that benefit from the formation of a transient polymer network having one set of properties and a final polymer network with distinctly different properties. Despite the range of applications, the robustness of this approach is demonstrated simply by optimizing the thiol:acrylate ratio in the initial formulation while using the same thiol and acrylic monomers in each formulation. The demonstrations of this approach will include a shape memory polymer, a lithographic impression material, and an optical material that serves as a substrate in which to write refractive index patterns. For shape memory polymers, fundamental to the change in shape is a concomitant decrease in modulus of several orders of magnitude as the polymer transitions from the glassy to the rubbery state. For impression materials, the challenge is associated with materials that are soft and exhibit low shrinkage during the impression stage while also exhibiting high strength and durability in the final stage as these two properties are inversely related. For writing refractive index gradients in optical polymers, low modulus is required to maximize diffusion of the high refractive index material. This same low modulus state renders the material difficult to handle and vulnerable to environmental contaminants necessitating secondary containment. Here, by utilizing a two-stage reactive polymer network forming system, the fundamental drawbacks of all three of these applications are uniquely addressed by maintaining the idealized properties desired for processing at the end of the initial curing stage while subsequently generating an idealized and orthogonal set of polymer properties for the ultimate application after the final curing step.

1.1. Shape Memory Polymers

A shape memory polymer (SMP) network is one with the unique ability to transition from a temporary, stored shape to a permanent shape upon the application of a stimulus such as temperature or light.[16–19] This shape change capacity is routinely exploited in minimally invasive biomedical applications in devices such as stents, endovascular coils, and orthopedic trauma fixation devices where the formation of a compressed state enables the device to be delivered through an opening that it would not otherwise fit through in its final, end application shape and state.[18] For biomedical systems, the trigger that is routinely applied to promote the final deployment is that of a temperature increase associated with the difference between ambient (or sub-ambient for refrigerated materials) and physiological temperatures. Thus, to perform as shape memory devices for biomedical applications, the glass transition temperature is typically near physiological temperature (i.e., 38 °C) which, for traditional materials necessitates a softening of the material and a reduction in the modulus in its deployed state, typically in the range of 1–23 MPa.[18] This behavior implies that a limitation of biomedical shape memory polymer systems is their lack of mechanical strength and modulus after being deployed in the body due to the necessity of performing while in or near the rubbery regime. In contrast to SMPs, the mechanical strength of shape memory NiTinol medical devices are typically around 60 GPa.[20] NiTinol shape memory devices such as stents are currently used in minimally invasive treatment of aneurysms

and in orthopedic applications such as suture anchors, i.e., devices that require a high modulus to function effectively.[21] Generally, because of the fundamental limitations associated with the necessity of undergoing the glass transition, SMPs that are designed to have a high modulus in their rubbery regime often attain it at a cost of reduced strain capacities and compromised shape memory properties.[22–30] In particular, composite shape memory polymer systems have been seen to increase the overall mechanical strength and modulus of the polymer, but often do so at the expense of shape memory characteristics such as shape fixity and shape recovery.[16,23–28] This trade-off limits the potential biomedical applications for which SMPs can be used, where the ability of the device to be strained into its temporary geometry is an important feature.

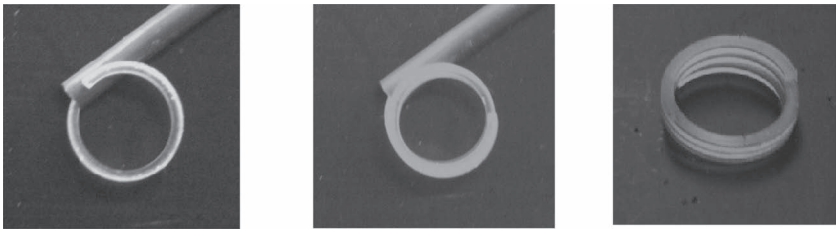

Figure 1. Shape memory polymer coils being deployed from a catheter: the coils begin at stage 1 and once the coils are deployed in their final shape, the second reaction (stage 2) can be initiated to increase the polymer modulus significantly.

Here, we developed dual-cure shape memory polymer system that exhibits an initial set of distinct mechanical properties suitable for deployment of a biomedical device and a second set of properties (high modulus) that are achieved in situ by a second stage curing that occurs after deployment and which are appropriate for the long-term success and function of the device (**Figure 1**).

1.2. Lithographic Impression Materials

There is an ever-present need to manufacture smaller devices at lower cost. As an alternative to Imprint Lithography which requires high temperatures for imprinting a pattern with micron and nano-scale resolution, step and flash imprint lithography (SFIL) has also been a successful technique for replicating intricate patterns at both the nano- and microscale in ambient conditions by utilizing UV light to cure the polymer resin while being pressed against a physical mask that contains submicrometer size features.[31–34] A challenge in this area for both nano- and micropatterning is finding an appropriate photopolymerizable material with low viscosity, low shrinkage, and the ability to form stable polymer networks that enable mold removal without loss of detail. Although soft and highly flexible molds such as those made from polydimethylsiloxane (PDMS) enable imprinting at reduced pressures, the elastomeric behavior of the polymer can result in a non-uniform negative being formed from the master pattern. Also, as PDMS will swell in most organic solvents that are used to lower its viscosity, this results in further distortion of the master pattern.[31] During the past few years, radical-mediated thiol-ene click reactions have been shown to perform as an excellent substrate for SFIL.[34] This soft lithography technique normally consists of pouring a liquid resin onto the pattern that is to be replicated and UV curing the resin on the patterned master. Once the polymer is cured, the thin film is peeled off the master pattern in a repeatable manner in which a large number of nano-imprints are produced from the same master pattern.

This study utilized the thiol-acrylate Michael addition reaction to form a stage 1 gel that is suitable as an imprint material (**Figure 2**). At the end of the stage 1 cure, a thiol-acrylate network is formed that can be used as the imprint material, which, as opposed to a liquid resin, would make this polymer impression material easier to handle and process. The physical master is pressed into the stage 1 material at ambient conditions and exposed to a UV source, where the stage 2 reaction is initiated. Once the material is fully cured, the patterned polymer is removed from the master, whereupon an imprint of the pattern is obtained.

1.3. Optical Materials

Optical devices formed by patterned refractive index variations in thick (⩾1 mm) solids are difficult to achieve via traditional photoresist methodologies.[35–37] Silver halide photographic emulsions can record holograms with sub-200-nm resolution, but these systems suffer from a need for solvent-based processing, swelling during wet processing, and film thicknesses that are limited to approximately 10 μm.[36] Dichromated gelatin (DCG) is another important holographic material and can achieve index contrasts of approximately 0.1 or greater.[37] However, in addition to requiring complex wet processing, these holograms are extremely sensitive to moisture and must

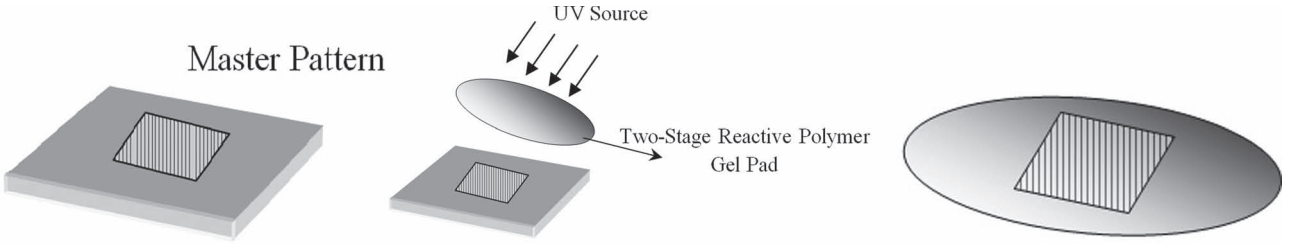

Figure 2. A master pattern with a micro-imprint pattern imprinted is utilized as a mold (a). Then the polymer gel pad that is formed after the stage 1 reaction is placed on the pattern block and UV cured (b). At the end of the stage 2 cure, the negative of the pattern is imprinted on the polymer pad (c).

be protected from ambient H_2O to remain stable. DCG can achieve index contrast of approximately 0.1 or greater but must be protected from ambient H_2O to remain stable. Self-developing photopolymers can achieve index variations of approximately 0.01 in films of several millimeters without necessitating any solvent-based processing.[38] Structured illumination initiates polymerization, locally depleting monomer and reducing free-volume. This approach drives diffusion of replacement monomer into and/or of binder out of the illuminated region, locally changing the density and the refractive index. After mass transport is completed, a uniform optical flood cure consumes the remaining photo-initiator and monomer, leaving an index-patterned, photoinsensitive structure that is stable to most environmental conditions.

This process must take place within a solid matrix that provides a physical scaffold for the photopolymer structure, allows rapid diffusion of low molecular-weight species, and has the required passive mechanical and optical properties. In "single-component" systems, this matrix is formed by optically or thermally polymerizing a single monomer past its gel point, leaving the remaining photoinitiator and monomer for structuring. Greater control over material properties is obtained by using a separate polymer to form the matrix in a "two-component" approach. Thin films can be solvent-cast with an inert binder while high quality volumes up to centimeter scale are possible with a thermosetting matrix formed via an orthogonal polymerization.[39,40]

These polymeric materials have been exploited for holographic data storage, optical filters, gradient index lenses, and waveguides.[41–44] However, both the single-component and two-component approaches have a fundamental problem for these applications in that the matrix, which must be above its glass transition temperature for efficient diffusion, remains so during operation. This rubbery matrix requires a sealed, solid enclosure to make it physically rigid and to suppress in-diffusion of environmental contaminants. Many applications are not compatible with this rubbery, high-diffusion state and instead require a final polymer that is mechanically and chemically robust. The approach reported here addresses this limitation by forming a first-stage polymer matrix with low glass transition temperature, followed by photopatterning the desired refractive index pattern, and ultimate crosslinking of the second-stage polymer to yield a glassy polymeric material.

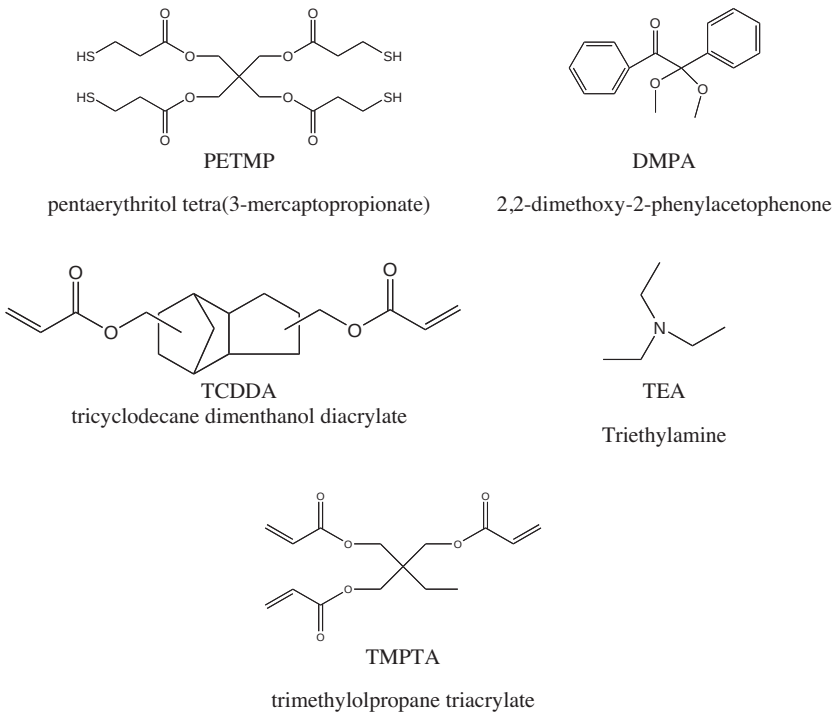

Figure 3. Chemical structures of the materials used in this study: a tetrathiol (PETMP), a diacrylate (TCDDA), a triacrylate (TMPTA), the radical initiator (DMPA), and the amine catalyst (TEA).

2. Results and Discussion

Thiol-acrylate polymer systems consisting of a tetrathiol (PETMP), a triacrylate (TMPTA), and a diacrylate (TCDDA) were designed to demonstrate the potential value of the dual cure behavior in a range of applications. The chemical structures of the monomers utilized in this work are given in **Figure 3**. Each of the application demonstrations comprises simple formulation manipulations; however, the differences in polymer properties and application potential are dramatic. To demonstrate this proof of concept, the thiol-acrylate systems were prepared with 1:1, 1:1.5, and 1:2 stoichiometric mixtures of thiol to acrylate functional groups, with the 1:1 systems serving as the control. Basic dual cure capability was demonstrated by evaluating functional group conversion, glass transition temperature, and modulus after both the first and second stages of polymerization. In the 1:1 systems, both the thiol and acrylate functional groups achieve nearly complete conversion in the first polymerization stage and no significant change in modulus or glass transition temperature was expected between the first and second stages of cure for the stoichiometric systems. **Table 1** and **2** shows conversions for each of the polymer systems after the stage 1 Michael addition reaction and the stage 2 acrylic homopolymerization. As expected, due to the click nature of the thiol-acrylate Michael addition, the thiol achieves nearly 100% conversion for all stoichiometric ratios during the stage 1 curing, and the stage 1 acrylate conversion is dictated by the stoichiometric amount of thiol initially present for this reaction stage. During the second stage of curing, the acrylate conversion increases significantly due to the radical-mediated homopolymerization.

Polymer glass transition temperature, T_g, and modulus are shown in **Table 3** and **4**. Both the 1:1.5 and 1:2 systems demonstrate a significant increase in both T_g and modulus during the second stage curing, in contrast to the minimal response in the 1:1 systems that serve essentially as controls. The control thiol-acrylate systems with 1:1 stoichiometric ratios represent

Table 1. Thiol and acrylate conversions after stage 1 and stage 2 curing. The PETMP/TMPTA samples contain varying stoichiometeric ratios of thiol to acrylate functional groups, with 0.8 wt% TEA to catalyze the stage 1 cure and 1 wt% Irgacure 651 for the stage 2 cure. A UV Black ray lamp with the power set to 8 mW cm^{-2} was used to initiate the stage 2 photopolymerization.

		Stage 1		Stage 2	
Formulation	Thiol-Acrylate Ratio	Thiol Conversion [%]	Acrylate Conversion [%]	Thiol Conversion [%]	Acrylate Conversion [%]
PETMP/TMPTA	1:1	97 ± 2	99 ± 1	97 ± 2	99 ± 1
	1:1.5	98 ± 2	57 ± 2	99 ± 1	98 ± 2
	1:2	96 ± 4	47 ± 2	95 ± 3	95 ± 5

Table 2. Thiol and acrylate conversions after stage 1 and stage 2 curing. The PETMP/TCDDA samples contain varying stoichiometeric ratios of thiol to acrylate functional groups, with 0.8 wt% TEA to catalyze the stage 1 cure and 1 wt% Irgacure 651 for the stage 2 cure. A UV black ray lamp with the power set to 8 mW cm^{-2} was used to initiate the stage 2 photopolymerization.

		Stage 1		Stage 2	
Formulation	Thiol-acrylate Ratio	Thiol Conversion [%]	Acrylate Conversion [%]	Thiol Conversion [%]	Acrylate Conversion [%]
PETMP/TCDDA	1:1	96 ± 3	98 ± 1	96 ± 3	99 ± 1
	1:1.5	94 ± 3	57 ± 1	97 ± 1	94 ± 1
	1:2	95 ± 1	46 ± 2	97± 2	97 ± 2

Table 3. Dynamic Mechanical Analysis (DMA) shows the distinct rubbery modulus and glass transition temperatures attained at the end of Stage1 and Stage 2 for the PETMP/TMPTA dual-cure polymer systems. The rubbery modulus was measured at T_g + 35 °C at the end of Stage 1 and T_g + 65 °C at the end of Stage 2.

		Stage 1		Stage 2	
Formulation	Thiol-Acrylate Ratio	T_g [°C]	Rubbery Modulus [MPa]	T_g [°C]	Rubbery Modulus [MPa]
PETMP/TMPTA	1:1	22 ± 3	22 ± 5	22 ± 2	20 ± 5
	1.5:1	9 ± 3	14 ± 2	41 ± 6	45 ± 10
	2:1	2 ± 1	9 ± 1	67 ± 2	81 ± 6

Table 4. DMA shows the distinct rubbery modulus and glass transition temperatures attained at the end of Stage 1 and Stage 2 for the PETMP/TCDDA dual-cure polymer systems. The rubbery modulus was measured at T_g + 35 °C at the end of stage 1 and T_g + 65 °C at the end of Stage 2.

		Stage 1		Stage 2	
Formulation	Thiol-Acrylate Ratio	T_g [°C]	Rubbery Modulus [MPa]	T_g [°C]	Rubbery Modulus [MPa]
PETMP/TCDDA	1:1	16 ± 2	7 ± 1	15 ± 1	8 ± 1
	1.5:1	4 ± 2	5 ± 1	27 ± 3	16 ± 2
	2:1	–6 ± 2	2 ± 1	46 ± 2	23 ± 1

the highest achievable T_g and modulus for a given set of monomers at the end of stage 1; however, these polymers also represent a minimum for the stage 2 modulus and glass transition temperature.

Stage 1 systems exhibited a T_g of 22 °C for the PETMP/TMPTA system and 15 °C for the PETMP/TCDDA system. Increasing the amount of acrylate reduces the initial T_g to 2 °C and –6 °C, respectively, for the 1:1.5 and 1:2 systems. The excess acrylate in these systems reduces the stage 1 T_g and modulus values, but when stage 2 curing is enabled, this difference results in dramatic increases in T_g and modulus with the 1:2 systems showing the greatest increase in modulus due to the presence of the greatest amount of unreacted acrylate available for curing in the second stage. The response seen during second stage curing is directly related to the amount of acrylate functional groups remaining after the first reaction.

Polymer properties, such as glass transition temperature and modulus were characterized for the samples using DMA, as shown in **Table 4** and **5**. All experimental systems showed a significant increase in both T_g and modulus during the second stage curing.

Modulus versus irradiation time is shown in **Figure 4** where the modulus evolution is compared for the 1:1.5 and 1:2 PETMP-TCDDA and PETMP-TMPTA systems. For the 1:2 systems, the initial modulus is lower than the 1:1.5 system due to the reduced amount of stage 1 curing; however, the subsequent increase in modulus was notably more dramatic, and ultimately, a higher final modulus is achieved. The results show

Table 5. Thermomechanical shape memory characterization data for two stage reactive SMP system.

Formulation	Stage 1 T_g [°C]	Stage 1 Rubbery Modulus [MPa]	Stage 2 T_g [°C]	Stage 2 Rubbery Modulus [MPa]	Stage 2 Modulus At 38 °C [MPa]	Free Strain Recovery [%]	Shape Fixity [%]	Shape Recovery Sharpness [%/C]
PETMP/TCDDA/ Ebecryl1290, 1:0.8:1.5 stoichiometric ratio	30 ± 3	21 ± 1	95 ± 8	64 ±8	1520 ± 60	96 ± 1	97 ± 1	3 ± 1

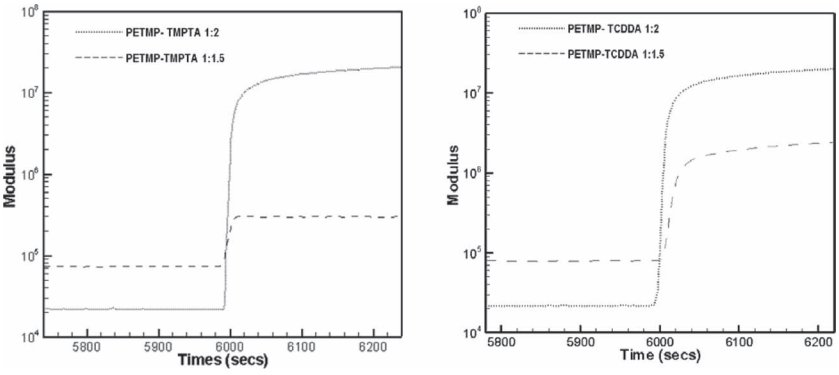

Figure 4. Rheology results showing the evolution of modulus from stage 1 to stage 2 cure for the PETMP-TMPTA system and the PETMP-TCDDA system. After the stage 1 cure, at 6000 s, the exposure to UV light causes radical-mediated acrylate polymerization and a corresponding increase in the modulus.

that as the acrylate to thiol ratio increases, the modulus for the first stage polymer decreases, while the modulus for the second stage polymer increases.

The results demonstrate that both stage 1 and stage 2 polymer properties can be engineered into the polymer network by incorporating simple formulation manipulations related to the monomer type, functionality, and stoichiometric ratio with initial stage 1 T_g and modulus values ranging from –6 °C to 2 °C and 2 to 9 MPa and stage 2 T_g and modulus values ranging from 46 °C to 67 °C and 23 to 81 MPa. To demonstrate the utility of the independent stage 1 and stage 2 properties, three proof of concept application examples are presented with dramatically different requirements for stage 1 properties and processing and final stage 2 properties. As discussed previously, these target applications are shape memory polymers, impression materials, and optical materials.

2.1. Shape Memory Polymers

To formulate a SMP system, a hexafunctional urethane acrylate (Ebecryl 1290) was incorporated into the monomer resin with the PETMP and TCDDA. Urethane acrylates have been shown to impart improved toughness to polymer networks and also have a history of use in shape memory polymers and a record of proven biocompatibility[16,17]. The theoretical gel point of this off-stoichiometric system with a thiol to acrylate ratio of 1 to 1.15 was calculated from the Flory–Stockmayer equation to be 0.30. The stage 1 reaction forms a shape memory polymer network with initial properties including a 33 °C T_g and a 20 MPa, modulus, that make it a potential polymer system for both biomedical and non-biomedical applications that require a low modulus, high strain shape memory material that can be easily programmed and confined to its temporary shape. Once the shape memory device has been deployed and is in its permanent configuration, the stage 2 reaction is initiated via UV irradiation and the remaining acrylate functional groups are photopolymerized to achieve the desired stage 2 material properties in situ.

The system utilized here exhibited a stage 2 T_g of 95 °C. After the stage 2 cure of the system, at 38 °C the system had a modulus of 1500 MPa. The high stage 2 modulus at physiological temperature enables the SMP to be used for potential new applications such as orthopedic devices in which the low modulus of SMPs in their deployed state has prevented them from being used in the past. To characterize this shape memory polymer system fully, free strain recovery, shape fixity, and shape recovery sharpness were evaluated and are presented in Table 5. Free strain recovery is a measure of the ability of the polymer system to recover its permanent shape in the absence of mechanical load as a function of increasing temperature or time. The SMP system showed a free strain recovery of 95%, and this response compares with other SMP system, where strain recovery typically falls between 90 and 100%.[16]

The shape fixity of a polymer system is an indication of the ability of the polymer network to store a temporary shape at a temperature that is below its transition region. In terms of applications, this measure is an indication of the material's ability to store strain energy within the polymer network before the device is activated. The polymer system consistently showed shape fixity of approximately 97%, which is compares favorably to other shape memory polymer systems, where shape fixity ranges between 80 and 100%.[16,30]

The shape recovery sharpness gives an indication of the breadth of the transition within which the polymer system would go from its temporary stored shape to its permanent shape. Larger shape recovery sharpness and a narrow strain recovery transition width indicate a rapid transition of the polymer from its stored shape to its final shape. Other SMP systems have been found to exhibit recovery sharpness values that range from 1.8 to 4.2% °C^{-1}.[16] Compared to these polymers, the systems formulated here demonstrated a relatively rapid recovery level of 3% °C^{-1} as shown in Table 5.

2.2. Impression Materials

The same thiol-acrylate monomers that were utilized in the SMP system, but in differing stoichiometric ratios, were used

Table 6. Thermomechanical characterization of the two stage impression lithography polymer.

Formulation	Stage 1 T_g [°C]	Stage 1 Rubbery Modulus [MPa]	Stage 2 T_g [°C]	Stage 2 Rubbery Modulus [MPa]
PETMP/TCDDA/Ebecryl1290 1:10:4 stoichiometric ratio	−10 ± 4	0.5 ± 0.2	195 ± 10	200 ± 20

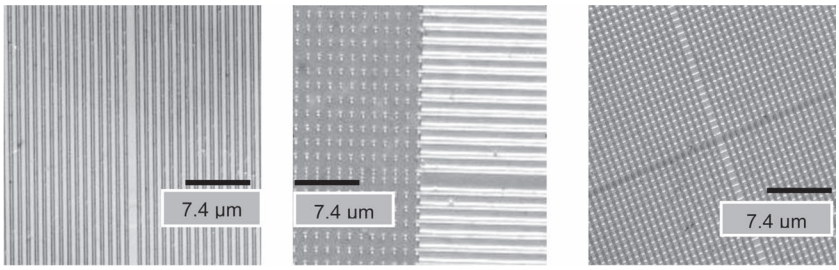

Figure 5. Brightfield images of the lithography pattern obtained from the two-stage polymer gel after stage 2 curing. The polymer film obtained at the end of stage 1 was used as a substrate to imprint the pattern from the mold and was then irradiated at 8 mW cm^{-2} for 5 min.

to formulate a polymer system for a lithographic/impression gel. In this formulation the thiol to acrylate stoichiometry was 1:7. Based off of the Flory–Stockmayer equation, the gel point conversion of this off-stoichiometric system was calculated to be 0.76. The results for T_g and modulus at the end of the stage 1 and stage 2 reactions are detailed in **Table 6**. The polymer that was formed at the end of stage 1 was used to take the imprint of a micron-sized pattern mold. Once the gel was formed, the physical mask was placed in contact with the polymer film and exposed to light at 8 mW cm^{-2} for 5 min, after which the stage 2 polymer was removed and brightfield images of the imprinted pattern were obtained. As shown in **Figure 5**, excellent negatives of the pattern from the mold were obtained in which the width of the structure matched that of the mold.

2.3. Optical Materials

In this third application, we have demonstrated a dual–cure system formulation for optical systems that comprises an initial 3:1 ratio of acrylate to thiol functional groups. The system contains PETMP, TCDDA and Ebecryl 1290 along with 5 wt% of a high refractive index monomer 2,4,6 tribromophenyl acrylate. The theoretical gel point conversion of the base system was calculated to be 0.58 from the Flory–Stockmayer equation. The high refractive index monomer is incorporated to facilitate the formation of areas with higher refractive index than the base system, thereby generating refractive index patterns that mirror the stage 2 light exposure pattern. The results for T_g and modulus at the end of the stage 1 and stage 2 reactions are detailed in **Table 7**. The dual-cure material system at the end of stage 1 was exposed to a holographic writing setup using a 365 nm argon laser. The collimated laser beam is split into two beams and redirected to interfere in the recording material with a spatial period of 2 µm. Following the stage 1 curing, two sequential exposures of the material are implemented in stage 2, the first being a patterned exposure to create the refractive index pattern and the second being a uniform (i.e., flood) curing to react the polymer fully. Here, the flood cure step was initiated by exposing the material to UV light at 8 mW cm^{-2} for 5 min. Differential interference contrast (DIC) phase images of the recorded grating were obtained and the pitch of the grating was measured at 2 µm, which matched with the holographic writing setup (**Figure 6**).

3. Conclusions

In this work we have demonstrated a two-stage network forming polymer system that serves as a materials platform for creating polymer systems with distinct stage 1 and stage 2 properties.

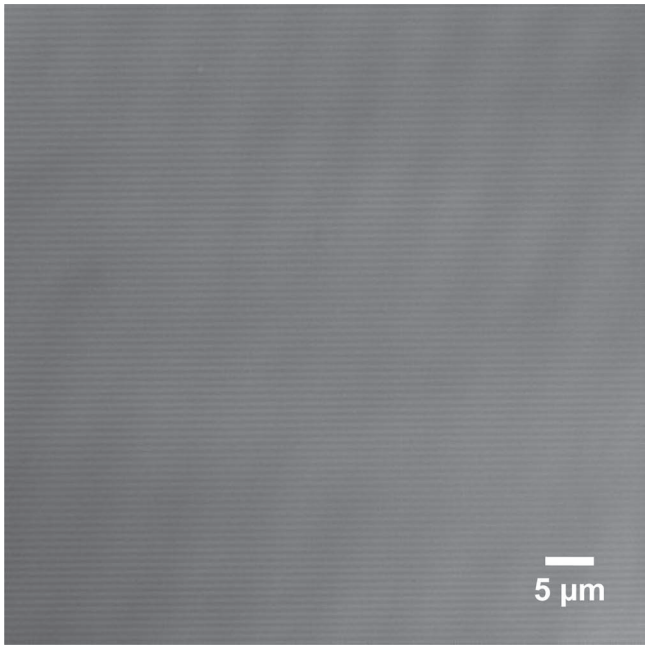

Figure 6. The image above is that of a hologram image recorded on the dual-cure polymer matrix. The stage 1 polymer was used as a photoresist to capture the interference pattern that was recorded on it. The diffraction grating is seen as a result of interference, indicating a refractive index gradient that was then imaged on a brightfield microscope.

Table 7. Thermomechanical characterization of the two stage holographic polymer material.

Formulation	Stage 1 T_g [°C]	Stage 1 Rubbery Modulus [MPa]	Stage 2 T_g [°C]	Stage 2 Rubbery Modulus [MPa]
PETMP/TCDDA/Ebecryl1290, 1:6:0.15 stoichiometric ratio	30 ± 4	6 ± 1	90 ± 10	45 ± 4

The polymer networks for both stage 1 and stage 2 are achieved orthogonally to each other such that additional polymer processing can occur after stage 1 curing to enable the attainment of two largely independent sets of material properties at different stages of the material processing and application lifetime. The ability to achieve a wide range of properties for both the stage 1 and stage 2 polymers enables a wide range of potential applications including the potential demonstrated here for high modulus shape memory polymers, lithographic impression materials, and optical materials with controlled refractive index patterns.

4. Experimental Section

Materials: Pentaerythritol tetra(3-mercaptopropionate) (PETMP) was donated by Bruno Bock, tricyclodecane dimethanol acrylate (TCDDA) was donated by Sartomer, and Ebecryl 1290 was donated by Cytec. Trimethylolpropane triacrylate (TMPTA) was purchased from Sigma-Aldrich. The photoinitiator Irgacure 651 (2,2-dimethoxy-2-phenylacetophenone) was donated by Ciba Specialty Chemicals. All samples contained triethyl amine (0.8 wt%) as a catalyst for the first stage reaction and Irgacure 651(1 wt%) to initiate the second reaction. Triethyl amine and Irgacure 651 were added to the thiol and mixed thoroughly. The acrylates were then added to the thiol and mixed vigorously on a vortex mixer. Although nucleophilic catalysts such as alkylarylphosphines have been shown to rapidly initiate and complete the Michael addition reaction efficiently, triethylamine was chosen for this study for the control it afforded over the initial rate of the reaction, allowing processing time while the monomer mixture could be subject to molding.[7–9] For the photopolymerization during the second stage of the reaction, samples were cured at 8 mW cm^{-2} using a UV lamp (Black-Ray Model B100AP). The formulations for the shape memory polymer material, the impression material and the optical holographic material contained PETMP/TCDDA/Ebecryl1290 at 1/0.8/1.5, 1/10/4, and 1/6/0.15 ratios of thiol and acrylate functional groups, respectively.

Dynamic Mechanical Analysis (DMA): DMA experiments were performed using a TA Instruments Q800 DMA.

Glass Transition Temperature: T_g was determined from polymer samples with dimensions of 10 mm × 3.5 mm × 1 mm. The sample temperature was ramped at 3 °C min^{-1} from –50 to 300 °C with a frequency of 1 Hz and a strain of 0.01% in tension. The T_g was assigned as the temperature at the tan δ curve maximum. The rubbery modulus was measured at T_g + 35 at the end of stage 1 and T_g + 65 at the end of stage 2.

Free Strain Recovery, Shape Fixity, and Shape Recovery Sharpness: Free strain recovery, shape fixity, and shape recovery sharpness were determined from fully cured samples with dimensions of 10 mm × 5 mm × 1 mm. For the free strain recovery tests, the polymers were held at a temperature 5 °C above the T_g of the system and strained in tension between 20 and 40% (always making sure to stay within the linear regime). The maximum strain was noted as ε_m. While maintaining the strain, the polymers were cooled to –25 °C at 20 °C per minute. The force was then maintained at zero and the strain on unloading the polymer was recorded (ε_u). The strain recovery was observed as the temperature was increased to 25 °C above the T_g at the rate of 3 °C min^{-1}. The final strain of the system post recovery was recorded as ε_p. Free strain recovery was defined as $R_r(\%) = (\varepsilon_u - \varepsilon_p)/(\varepsilon_m - \varepsilon_p) \times 100$. Shape fixity is given by $R_f(\%) = (\varepsilon_u/\varepsilon_m) \times 100$, and the shape recovery sharpness is defined by $v_r = R_r/\Delta T$, where ΔT is a measure of the width of the transition and is the temperature range from the onset of the recovery to its completion.

Polymer Coils: For the fabrication of polymer coils, a Teflon cylinder was inserted into a tight-fitting glass tube. The monomer mixture was added into the mold and the stage 1 cure was allowed to proceed for approximately 48 h. The glass tube was broken and the stage 1 polymer was carefully removed from the mold. For second stage curing, coils were photopolymerized using a UV lamp (Black-Ray Model B100AP) at 8 mW cm^{-2} for 10 min.

Fourier Transform Infrared Spectroscopy (FTIR): FTIR experiments were performed using a Nicolet Magna 760. Thiol peak absorbance was measured at 2570 cm^{-1} and acrylate peak absorbance was measured at 814 cm^{-1}. Samples were prepared and mounted between salt crystals, and spectra were taken before the addition of initiator (TEA), and the thiol and acrylate peak areas were recorded as A_{thiol} and $A_{acrylate}$, respectively. Samples were then prepared with TEA, mounted between salt crystals, and stored for 48 h to allow substantial time for the first stage curing. After 48 h, spectra were taken and the peak areas for the thiol and acrylate were recorded, both before and after exposure to UV light for 10 min. Thiol conversion was defined as $\alpha_{thiol} = 1 - ((A_{thiol})_{t = final}/(A_{thiol})_{t = initial})$. Acrylate conversion is given by $\alpha_{acrylate} = 1 - ((A_{acrylate})_{t = final}/(A_{acrylate})_{t = initial})$.

Rheology: Rheology experiments were performed using a TA Instruments ARES rheometer. Samples were prepared on 8 mm parallel geometry plates for dynamic testing. A dynamic time sweep test was performed using a strain of 0.2% and a frequency of 10 Hz, with data points being recorded once every second. The first stage was observed for up to 100 min after the monomers were mixed and then samples were concurrently exposed to UV light for 10 min at 8 mW cm^{-2} during testing. The evolution of the modulus from stage 1 to stage 2 was measured.

Acknowledgements

The authors would like to acknowledge National Science Foundation CBET 0626023, National Institute of Health T32HL072738, and the University of Colorado Technology Transfer Office CU2615B-01 for providing funding for this research.

Received: November 14, 2011
Published online: January 26, 2012

[1] A. R. Kannurpatti, K. J. Anderson, J. W. Anseth, C. N. Bowman, *J. Polym. Sci. Part B: Polym. Phys.* **1997**, *35*, 2297.
[2] C. N. Bowman, C. J. Kloxin, *AIChE J.* **2008**, *54*, 2774.
[3] A. F. Jacobine, *In Radiation Curing in Polymer Science and Technology III: Polymerization Mechanisms*, (Eds: J. D. Fouassier, J. F. Rabek), Elsevier, London **1993**, pp. 219–268.
[4] B. D. Mather, K. Viswanathan, K. M. Miller, T. E. Long, *Prog. Polym. Sci.* **2006**, *31*, 487.
[5] N. B. Cramer, C. N. Bowman, *J. Polym. Sci. Part A*, **2001**, *39*, 3311.
[6] C. E. Hoyle, C. N. Bowman, *Angew. Chem. Int. Ed.* **2010**, *49*, 1540.
[7] L. Qin, D. A. Wicks, C. E. Hoyle, *J. Polym. Sci., Part A: Polym.Chem.* **2007**, *45*, 5103.
[8] J. W. Chan, H. Wei, H. Zhou, C. E. Hoyle, *Eur. Polym. J.* **2009**, *45*, 2717.
[9] J. W. Chan, C. E. Hoyle, A. B. Lowe, *J. Am. Chem. Soc.* **2009**, *131*, 5751.
[10] J. W. Chan, C. E. Hoyle, A. B. Lowe, M. Bowman, *Macromolecules* **2010**, *43*, 6381.
[11] A. B. Lowe, *Polym. Chem.* **2010**, *1*, 17.
[12] C. E. Hoyle, T. Y. Lee, T. Roper, *J. Polym. Sci., Part A: Polym.Chem.* **2004**, *42*, 5301.
[13] D. L Elbert, A. B. Pratt, M. P. Lutolf, S. Halstenberg, J. A. Hubbell, *J. Controlled Release* **2004**, *76*, 11.
[14] A. M. Kloxin, M. Tibbitt, A. M. Kasko, J. A. Fairbairn, K. S. Anseth, *Adv. Mater.* **2010**, *22*, 61.
[15] A. E. Rydholm, C. N. Bowman, K. S. Anseth, *Biomaterials* **2005**, *26*, 4495.
[16] P. T. Mather, X Luo, I. A. Rousseau, *Annu. Rev. Mater. Res.* **2009**, *39*, 445.
[17] C. Liu, H. Qin, P. T Mather, *J. Mater. Chem.* **2007**, *17*, 1543.

[18] C. M. Yakacki, R. Shandas, D. Safranski, A. M. Ortega, K. Sassaman, K. Gall, *Adv. Funct. Mater.* **2008**, *18*, 2428.
[19] C. M. Yakacki, R. Shandas, C. Lanning, B. Rech, A. Eckstein, K. Gall, *Biomaterials* **2007**, *28*, 2255.
[20] A. Bezrouk, J. Hanus, J. Zahora, *Scripta Med.* **2005**, *78*, 219.
[21] T. W. Duerig, D. Stoeckel, A. Pelton, *Mater. Sci. Eng.* **1999**, *273*, 149.
[22] A. Lendlein, S. Kelch, *Angew. Chem. Int. Ed.* **2002**, *114*, 2138.
[23] I. A. Rousseau, *Polym. Eng. Sci.* **2008**, *48*, 2075.
[24] D. Ratna, J. Karger-kocsis, *J. Mater. Sci.* **2008**, *8*, 254.
[25] M. Y. Razzaq, L. Frormann, *Polym. Compos.* **2007**, *28*, 287.
[26] Q. H. Meng, J. F. Hu, *Compos. Part: App. Sci. Manu.* **2008**, *39*, 314.
[27] J. W. Xu, W. F. Shi, W. M. Pang, *Polymer* **2006**, *47*, 457–465.
[28] K. Gall, M. L. Dunn, Y. Liu, D. Finch, M. Lake, N. A. Munshi, *Acta Mater.* **2002**, *50*, 5115.
[29] T. Xie, I. A. Rousseau, *Polymer* **2009**, *50*, 1852.
[30] D. P. Nair, N. B. Cramer, T. F. Scott, C. N. Bowman, R. Shandas, *Polymer* **2010**, *51*, 4383.
[31] Y. Xia, G. M. Whitesides, *Angew. Chem. Int. Ed.* **1998**, *37*, 550.
[32] H. D. Rowland, W. P. King, *Appl. Phys. A: Mater. Sci. Process.* **2005**, *81*, 1331.
[33] T. C Bailey, S. C. Johnson, S. V. Sreenivasan, J. G. Ekerdt, C. G. Willson, D. J. Resnick, *J. Photopolym. Sci. Technol.* **2002**, *15*, 481.
[34] V. S. Khire, Y. Youngwoo, N. A. Clark, *Adv. Mater.* **2007**, *20*, 3308.
[35] R. R. A. Syms, *Practical Volume Holography*, Oxford University Press, Oxford, UK **1990**.
[36] V. W. Krongauz, A. D. Trifunac, *Processes In Photoreactive Photopolymers*, Chapman & Hall, New York **1994**.
[37] B. J. Chang, C. D. Leonard, *Appl. Opt.* **1979**, *48*, 2407.
[38] D. H. Close, A. D. Jacobson, R. C. Magerum, R. G. Brault, F. J. McClung, *Appl. Phys. Lett.* **1969**, *14*, 159.
[39] W. S. Colburn, K. A. Haines, *Appl. Opt.* **1971**, *10*, 1636.
[40] L. Dhar, A. Hale, H. E. Katz, M. L. Schilling, M. G. Schnoes, F. C. Schilling, *Opt. Lett.* **1999**, *24*, 487.
[41] K. Curtis, L. Dhar, A. Hill, W. Wilson, M. Ayres, in *Holographic Data Storage: From Theory to Practical Systems*, (Eds: K. Curtis, L. Dhar, A. Hill, W. Wilson, M. Ayres), Wiley, New York **2010**.
[42] A. Sato, M. Scepanovic, R. K. Kostuk, *Appl. Opt.* **2003**, *42*, 778.
[43] C. Ye, R. R. McLeod, *Opt. Lett.* **2008**, *33*, 2575.
[44] A. C. Sullivan, M. W. Grabowski, R. R. McLeod, *Appl. Opt.* **2007**, *46*, 295.